Superalloys 718, 625, 706 and Derivatives 2005 *Edited by E.A. Loria*
TMS (The Minerals, Metals & Materials Society), 2005

THERMOPHYSICAL PROPERTIES OF IN738LC, MM247LC AND CMSX-4 IN THE LIQUID AND HIGH TEMPERATURE SOLID PHASE

Ragnhild E. Aune[1], Livio Battezzati[2], Robert Brooks[3], Ivan Egry[4], Hans-Jörg Fecht[5], Jean-Paul Garandet[6], Miyuki Hayashi[1], Ken C. Mills[7], Alberto Passerone[8], Peter N. Quested[3], Enrica Ricci[8], Frank Schmidt-Hohagen[4], Seshadri Seetharaman[1], Bernard Vinet[6], Rainer K. Wunderlich[5]

[1]KTH, Department of Materials Science and Engineering, 10044 Stockholm, Sweden
[2]Università degli Studi di Torino, Dipartimento di Chimica IFM, Via Pietro Giuria, 10125 Torino, Italy
[3]NPL, Materials Centre, Queens Road, Teddington, Middlesex TW11 OLW, UK
[4] DLR, ZEUS Center of Excellence, Linder Höhe, 51147 Cologne, Germany
[5]Materials Division, Ulm University, Albert-Einstein-Allee 47, 89081 Ulm, Germany
[6] CEA/CEREM, Departement des Technologies pour les Energies Nouvelles, 17 Rue des Martyrs, 38054 Grenoble Cédex 9, France
[7]Imperial College STM, Department of Materials, Prince Consort Road, London, SW7 2BP, UK
[8]IENI-CNR Department of Genova, Via de Marini, 16149 Genova, Italy

ABSTRACT

Thermophysical properties of the Ni-based superalloys *CMSX-4*, *IN738LC,* and *MM247LC* have been measured in the liquid and high-temperature solid phase. Properties included calorimetric, thermal transport, the surface tension, and the viscosity. Experiments have been performed in ground-based laboratory using classical calorimetry and rheometry as well as under reduced gravity conditions in an electromagnetic levitation device on board parabolic flights. In this contribution, an overview of the various properties of three *Ni*-based superalloys is given with emphasis on the surface tension and viscosity as obtained from the parabolic flight experiments. The measurements were performed within a program called *ThermoLab* dedicated to the measurement of thermophysical properties of industrial alloys.

Introduction

Modelling of casting and solidification processes is becoming of widespread use in the industry[1] and commercial software tools are now available to this purpose allowing improved efficiency in materials design [2]. The application of this programme is often hampered by the lack of reliable thermophysical property values of liquid metals which are needed as input parameters for the computational models [3]. In this respect, there is a discrepancy between the ever increasing sophistication of the calculational models and computer power, and the availability or accuracy of the thermophysical property values in the liquid phase. The paucity of thermophysical property data is owed to the high chemical reactivity of many metallic alloys in the liquid phase. This holds in particular for high-temperature alloys such as *Ti* alloys and *Ni*-based superalloys but also for some low-temperature light-weight alloys such as the *Mg* and *Li* alloys, which are of interest to the automotive industries. For many metallic alloys of technological relevance, this chemical reactivity will affect the results of thermophysical property measurements where the liquid is in contact with a containing surface, or will make these measurements impossible altogether. Moreover, due to the high oxygen affinity of many liquid metals, the processing atmosphere may affect the outcome of measurements of properties like the surface tension or the viscosity.

The *ThermoLab* project aims at providing high-quality data for thermophysical properties related to the numerical modelling of industrial casting and solidification processes. The program includes thermophysical property measurement in ground-based laboratory using classical calorimetric and rheological techniques as well as containerless methods based on electomagnetic levitation under reduced gravity conditions [4]. In addition, the project is concerned with the thermodynamic modelling of thermophysical properties. In this contribution, an overview is given of typical thermophysical property values of *Ni*-based superalloys obtained in this program with emphasis on the surface tension and viscosity obtained by the oscillating drop method under reduced gravity conditions on board parabolic flights.

Experimental Elements

The *ThermoLab* project endeavors to provide an as complete as possible thermophysical characterization of a variety of industrial alloys. The feasibility of this goal using conventional thermoanalytical equipment -- where the specimen are in contact with a containing surface -- depends on the alloys and the properties to be investigated. For the *Ni*-based superalloys container wall reactions, for example, in classical calorimetric devices are not as critical as, for instance, for *Ti*-alloys. However, properties like the surface tension which is rather sensitive to the presence of surface active elements may be more susceptible to contamination from container reactions. Thus, the *ThermoLab* project tries to combine whenever possible classical thermoanalytic methods with containerless processing techniques based on electromagnetic levitation and, in addition, use a reduced gravity environment whenever this particular property is required for a certain measurement technique which can not be performed quantitatively in ground-based electromagnetic levitation[5]. One such property is the viscosity which in ground-based electromagnetic levitation can not be measured by oscillating drop method because of the presence of turbulent fluid flow in the specimen [6]. Here, we describe in short measurements of the surface tension and the viscosity by the oscillating drop method in an electromagnetic levitation device as have been performed in a series of parabolic flight experiments.

Parabolic flights provide about twenty seconds of reduced gravity. The specimen is positioned by an electromagnetic quadrupole field, and inductively heated by a dipole field of frequencies 240 and 320 kHz, respectively. The twenty seconds of reduced gravity are sufficient to melt, heat a specimen into the liquid phase, and cool to solidification. In the cooling phase after the heating field is turned off, magnetic field pulses are applied to excite surface oscillations. These pulses have durations of typically 0.10 - 0.30 seconds. In Figure 1, the temperature-time profile of processing a *CMSX-4* specimen on a parabolic flight is shown with 1: melting and heating into the liquid phase; 2: cooling after turning off the heater field; 3: excitation of surface oscillations by magnetic field pulses; 4: solidification.

The frequency and the damping time constant are evaluated from the optical recording of the specimen shape by two 100 Hz frame rate analog cameras in the top and radial position with the top position defined by the axis of the dipole field. In the meanwhile the 100 Hz frame rate analog cameras have been replaced by 150 Hz digital image recording cameras. The frames from the analog recordings were digitized and

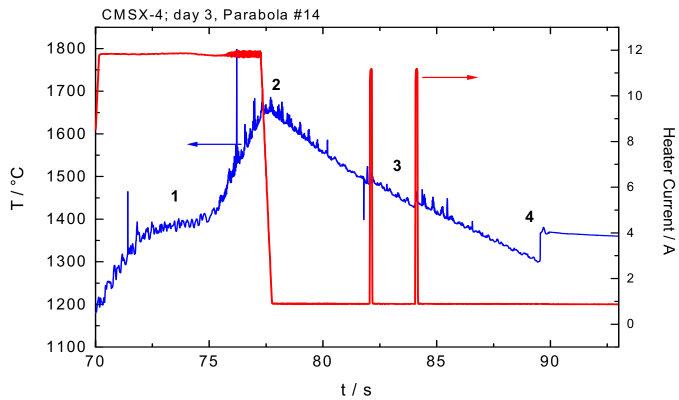

Figure 1. Temperature – time profile, left hand ordinate, of a *CMSX-4* specimen in the reduced gravity phase of a parabolic flight. The current in the rf- heater generator is shown on the right hand ordinate.

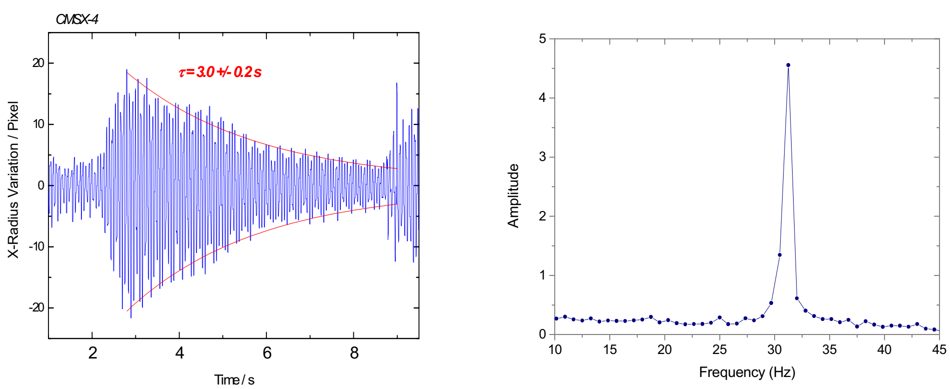

Figure 2a,b. Variation of the radius of a *CMSX-4* specimen as a function of time after excitation of surface oscillations by a magnetic field pulse. 2b. Fourier analysis of a 1.24 second time slice of the radius variation shown in Figure 2a.

analyzed by a dedicated software. In Figure 2a, the time variation of the specimen diameter is shown, and in Figure 2b, the Fourier transform of a 1.24 second time slice. The spectrum exhibits a single peak as it is to be expected for a non-rotating force free non-rotating specimen. Under force-free conditions, the surface tension σ can be evaluated from the oscillation frequency ν according to the Raleigh formula:

$$\sigma = \frac{3}{8}\pi \nu^2 M \tag{1}$$

with M the specimen mass. The viscosity is evaluated from the damping time constant τ of the surface oscillations with R the specimen radius:

$$\eta = \frac{3}{20\pi}\frac{M}{R}\tau^{-1} \tag{2}$$

The optical recording of the specimen shape allows the evaluation of the center of gravity movement from which the Cummings[7] correction of the Raleigh frequency can be derived. Under the condition of the parabolic flight, the Cummings correction originating from the magnetic field pressure of the position field amounts to at most a reduction of 2 % of the value of the surface tension at the liquidus temperature.

Results

Calorimetric Properties

In Table I , the solidus and liquidus temperatures and of the enthalpy of fusion of the alloys investigated are shown. The numbers present an average of results obtained in three different laboratories by high temperature calorimetry. The results from the three participating laboratories agreed within 5 K. Liquidus temperatures were obtained from heating rate dependent measurements and extrapolating to zero heating rate. The solidus temperatures were obtained from the onset of melting on heating because the specimen exhibited a variable degree of undercooling as shown in the DSC trace of Figure 3 for the alloy *MM247LC* heated and cooled with R = 20 K/min.

The enthalpy of fusion was obtained by comparison of the HTDSC melting curve area with the one of high purity *Ni* and, by scaling of the calorimeter sensitivity curve from

Table I: Basic calorimetric properties of some *Ni*-based superalloys

Alloy	T_s/°C	T_l/°C	ΔH_f / Jg^{-1}
CMSX-4	1312 ± 5	1382 ± 2	231 ± 12
MM247LC	1282 ± 6	1368 ± 2	264 ± 8
IN738LC	1269 ± 6	1325 ± 4	248 ± 8

the melting temperature of *Ni* to the liquidus temperature of the alloy. This correction resulted typically in a reduction of the measured enthalpy of fusion by 8 % because the sensitivity of the calorimeters is a decreasing function of temperature.

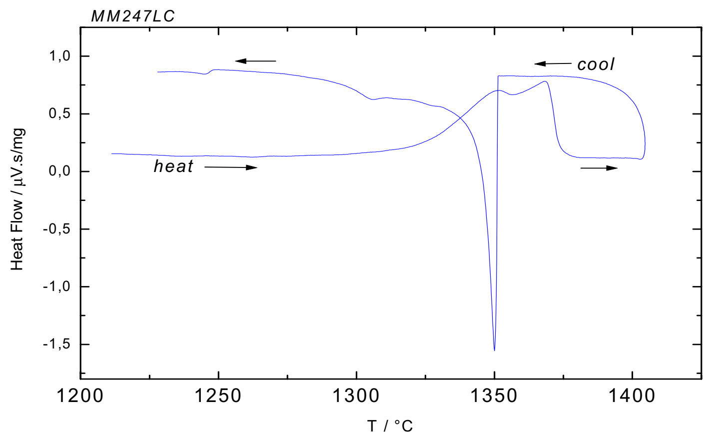

Figure 3: DSC traces of heating and cooling a
MM247LC specimen with $R_{H,C}$ = 20K/min.

The fraction solid as a function of temperature is an important parameter in solidification modelling. Its measurement, on solidification is, however, complicated by the presence of a variable degree of cooling rate dependent undercooling. In Figure 4, the fraction solid on heating is shown for different heating rates. The curve termed "0 °C/min" is the result of an extrapolation procedure. The temperatures at which a given solid fraction occurs at various heating rates were linearly fitted and extrapolated to zero rate. The set of temperatures obtained was then fitted using a polynomial, resulting in the curve labelled "0 °C/min". This procedure is suitable to determine the solid fraction corresponding to the equilibrium phase diagram.

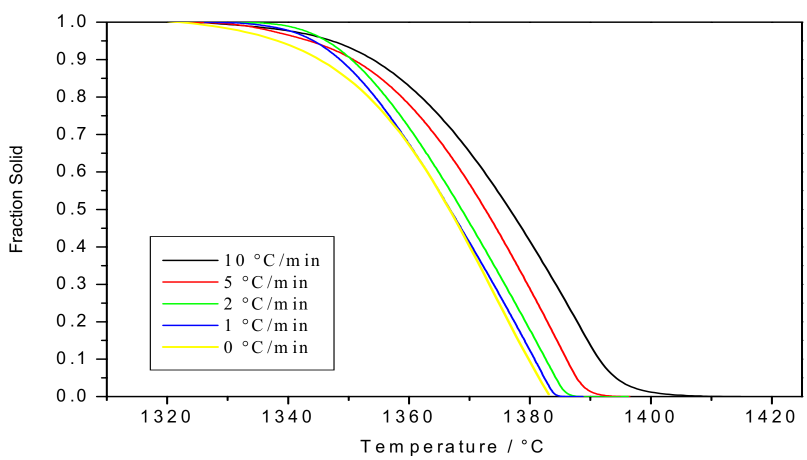

Figure 4: *CMSX-4*, solid fraction traces on heating at different rates

Thermal Diffusivity of *CMSX-4*

The thermal diffusivity of *CMSX-4* was measured in the liquid and the solid phase by the laser flash method. The thermal diffusivity in the solid phase as a function of temperature is shown in Figure 5. Measurements were performed during the heating cycle at first and then during the cooling cycle at intervals of 100 K over the temperature range between room temperature and the temperature just below the liquidus temperature. The measurement was repeated three times at each temperature, and four runs were carried out to confirm the reproducibility.

Thermal diffusivity is a structure sensitive property. As such, it is expected to depend on the thermal history of the experiment because of the sluggish structural changes. In order to investigate the effect of the thermal history on the thermal diffusivity, isothermal annealing measurements were performed. The sample was kept at 1573 K, 1403 and 1277 K for 12 hrs, and the time evolution of the thermal diffusivity was measured. Variations of about 10 % were observed on a timescale of 1 – 8 hrs annealing time which is related to structural changes. At the lower annealing temperatures, a coarsening of the γ' phase was observed in SEM. The thermal diffusivity, λ, of *CMSX-4* in the liquid phase exhibits a constant value in the

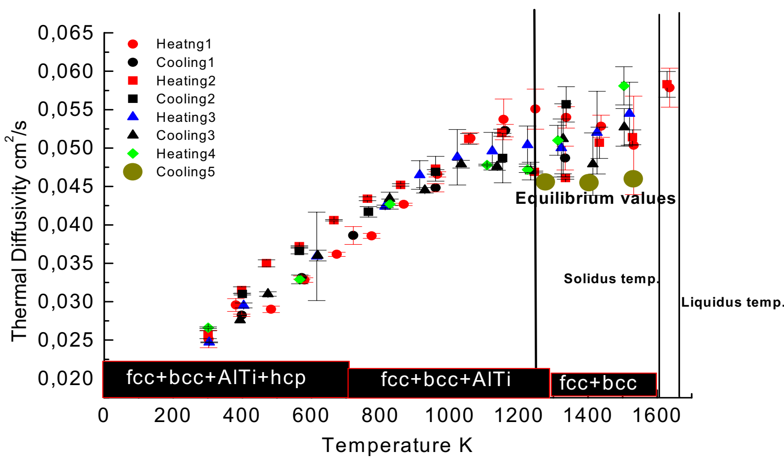

Figure 5. Thermal diffusivity in the solid phase of *CMSX-4*.

temperature range from 1480 – 1580 °C of $\lambda = 0.0582$ cm^2 s^{-1}. With a specific heat capacity in the liquid phase of $c^l_P = 0.70 \pm 0.03$ JK^{-1}g^{-1} and a density of 8.058 g cm^{-3}, the average thermal conductivity κ in the liquid phase in the temperature range 1480 – 1580 °C is obtained as $\kappa = 0.328$ W K^{-1} cm^{-1}. With the Wiedemann-Franz law, this results in an average electrical resistivity in this temperature range of 133 µΩcm which is a very reasonable number for a transition metal melt. The density was obtained in ground based electromagnetic levitation by optical methods, and the specific heat capacity was obtained by classical high temperature calorimetry.

<u>Surface Tension From Parabolic Flights</u>

The surface tension of *CMSX-4* as a function of temperature obtained from the parabolic flight experiments is shown in Figure 6. The oxygen concentration of the specimen prepared for the parabolic flight and of the processed specimen were analyzed by the LECO hot gas extraction method giving 43 and 51 wt ppm oxygen, respecitely. In Table II, an overview of the surface tensions and the temperature coefficients of the *Ni*-based superalloys processed in the *ThermoLab* parabolic flight programme is shown.

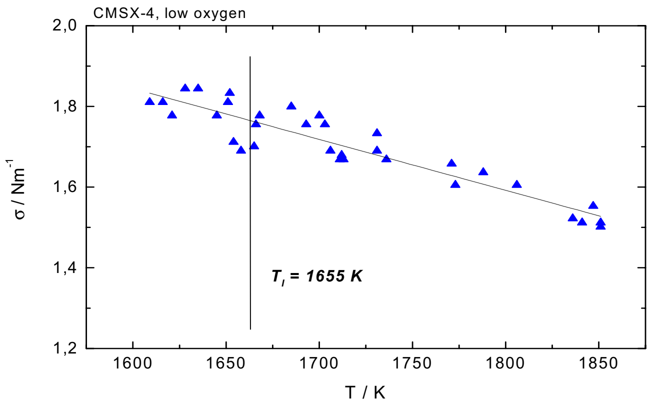

Figure 6: Surface tension of *CMSX-4* as a function of temperature obtained from parabolic flight experiments.

In the table, there are also included two values of the surface tension of *CMSX-4*, obtained in ground-based experiments by the sessile drop method. The variation in the values of the surface tension between the different experiments demonstrates the importance of strict processing atmosphere control with regard to the concentration of

Table II: Surface tension at the liquidus temperature and temperature coefficient

Alloy	T_l / °C	σ (T_l) Nm^{-1}	$d\sigma$ / dT Nm^{-1} K^{-1}	Method
CMSX-4	1384	1.77	$-1.37\ 10^{-3}$	oscillating drop parabolic flight
CMSX-4	1384	1.97	$-1.38\ 10^{-3}$	sessile drop
CMSX-4	1384	1.82	$-1.42\ 10^{-3}$	sessile drop
IN738LC	1335	1.85	$-1.48\ 10^{-3}$	oscillating drop parabolic flight
MM247LC	1368	1.86	$-1.36\ 10^{-3}$	oscillating drop parabolic flight
C263	1368	1.74	$-6.85\ 10^{-4}$	oscillating drop parabolic flight

surface active elements such as oxygen. Because the oxygen concentration of the specimen processed on the parabolic flight is close to that of the starting concentration the value obtained from the parabolic flight experiments is considered as the best available.

Viscosity from Parabolic Flight Experiments

The viscosity from the parabolic flight experiments was evaluated from the damping time constant of surface oscillations as shown in Figure 2 and Eq. 2. In Figure , an Arrhenius plot of the viscosity of the IN738LC alloy is shown according to:

$$ln\ \eta(T) = ln\ \eta_o + \Delta E_a / k_B T \qquad (3)$$

with η_o the prefactor and ΔE_a the activation energy for viscous flow.

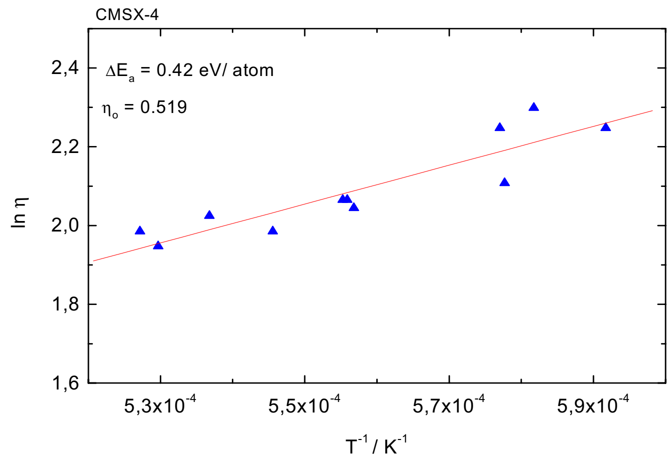

Figure 7: Arrhenius plot of the viscosity of *IN738LC*.

In Table III, the constants of the Arrhenius plots of the viscosities of the alloys *CMSX-4*, *MM247LC* , *IN738LC* and *C263* are shown.

Table III: Arrhenius constants of the viscosity of some *Ni*-based superalloys.

Alloy	η_o / mPas.s	ΔE_a / eV atom^{-1}
CMSX-4	0.52	0.42
MM247LC	0.38	0.35
IN738LC	0.59	0.39
C263	1.044	0.31

Modelling

Thermodynamic Modelling of the surface tension

The *Ni-Al* bianary alloy system forms the basis of several more complex industrial alloys among these the Ni-based superalloys. It is, thus, of interest to have available models allowing to predict the surface tension and also the viscosity as a function of composition for a whole class of alloys. The modelling starts with the basic binary alloy which is then extended to the more complex industrial alloys. In Figure 8, the surface tension isotherm at T = 1640 °C of *Ni-Al* is shown for the different models.

Table IV: σ (exp: experimental values from parabolic flights.); σ (CFM) compound formation model; σ (Reg) regular solution model.

Alloy Composition	σ (exp) / Nm^{-1}	σ (CFM) / Nm^{-1}	σ (Reg) / Nm^{-1}
Al – 75at%Ni	1.52	1.65	1.41
Al – 65at%Ni	1.54	1.52	1.22
Al – 31.5at%Ni	0.801	0.98	0.81

The theoretical results are compared to experimental values of three different *Ni-Al* compositions obtained in a recent parabolic flight experiment as shown in Table IV. For 75 and 65 at%Ni agreement between the experimental and the values obtained with the CFM is very good, for 31.5 at% *Ni* the experimental value is closer to the prediction of the regular solution model. The measured values have been scaled to T = 1640 °C with the corresponding temperature coefficient. Extrapolations over such a large temperature range are sensitive to the value of the temperature coefficient of the surface tension. Because the coefficient is very sensitive to impurities these results have to be considered with some care. Recently, Hayashi et al. performed a calculation for *CMSX-4* based on the Buttler equation to obtain a value of $\sigma(T_l) = 1.776 \pm 0.050$ Nm^{-1} at $T_l = 1395$ °C, which is in very good agreement with the experimental value obtained in the parabolic flight experiment. Scaling of the surface tension of the *Al-65at%Ni* alloy to $T_l = 1395$ °C gives a value of $\sigma(T_l) = 1.79 \pm 0.050$ Nm^{-1}, which agrees quite well with the surface of *CMSX-4* at the liquidus temperature.

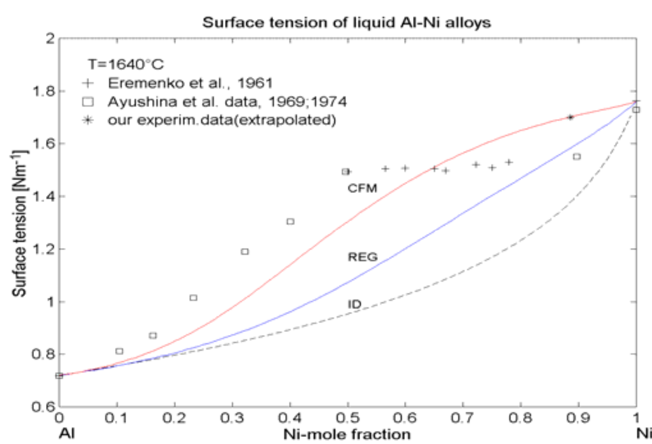

Figure 8: Surface tension isotherm of Ni-Al at T=1640°C.

Thermodynamic Calculations

In addition to the HTDSC measurements, numerical calculations of the various thermodynamic properties investigated have been performed for the *CMSX-4* alloy using the *ThermoCalc* program [6]. The most advanced commercial thermodynamic database, the *TTNi*-Data from Thermotech UK, has been employed in the calculations. This database includes almost every component present in the specimen, except *Mn*, *Si* and *Fe*. These latter elements have then been neglected in the calculations. The phase stability regions are shown in Figure 9.

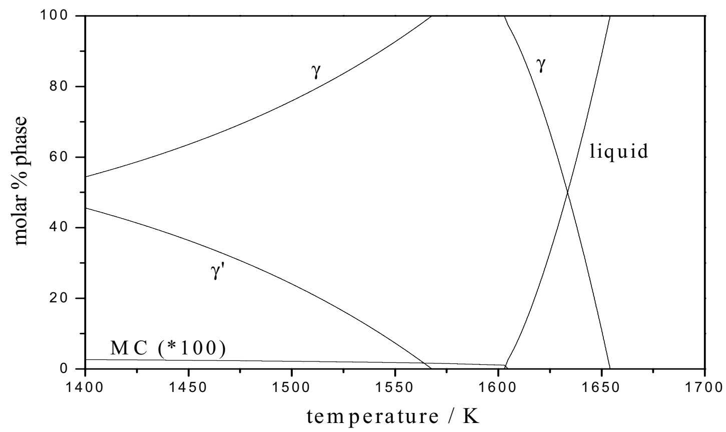

Figure 9: Calculated phase stability in CMSX-4.

References

1. J.A. Dantzig,"Solidification Modeling: State and Outlook, " *Journal of Metals,* **52** (2000), 18-21.

2. M. Rappaz, M. Rettenmayr, "Current Opinion," *Solid State & Materials Science,* 3 (1998), 275.

3 . A. Ludwig, "Thermophysical properties necessary for advanced casting simulations," *International Journal Thermophysics* **23** (2002), 1131-1146.

4. D. M. Herlach, R. F. Cochrane, I. Egry, H.-J. Fecht, and A. L. Greer, (1993). "Containerless processing in the study of metallic melts and their solidification," *International Materials Review* **38**, (1993) 273-347.

5 . R. K. Wunderlich and H.-J. Fecht, "Modulated electromagnetic induction calorimetry of reactive metallic liquids,", *Measurement Science and Technology.* **16**, 402-416.

6 . R. W. Hayers, "Fluid flow effects in levitated droplets" *Measurement Science and Technology.* **16**, 402-416.

7 . D. L. Cummings and D. A. Blackburn, "Oscillations of Magnetically Levitated Aspherical Droplets," *Journal of Fluid. Mechanics* **224** (1991) 395-416.